© 2014. Published by The Company of Biologists Ltd | Journal of Cell Science (2014) 127, 4024–4036 doi:10.1242/jcs.151910

RESEARCH ARTICLE

Septin ring assembly is regulated by Spt20, a structural subunit of the SAGA complex

Bingkun Lei[1,*], Nan Zhou[1,*], Yuchen Guo[1], Wenqi Zhao[2], Yan-Wen Tan[2], Yao Yu[1,3,‡] and Hong Lu[1,3,4,‡]

ABSTRACT

Accurate cell division requires the proper assembly of high-order septin structures. In fission yeast (*Schizosaccharomyces pombe*), Spn1–Spn4 are assembled into a primary septin ring at the division site, and the subsequent recruitment of Mid2 to the structure results in a stable septin ring. However, not much is known about the regulation of this key process. Here, we found that deletion of Spt20, a structural subunit of the Spt–Ada–Gcn5–acetyltransferase (SAGA) transcriptional activation complex, caused a severe cell separation defect. The defect was mainly due to impaired septin ring assembly, as 80% of *spt20*Δ cells lost septin rings at the division sites. Spt20 regulates septin ring assembly partially through the transcriptional activation of *mid2*$^{+}$. Spt20 also interacted with Spn2 and Mid2 *in vitro* and was associated with other components of the ring *in vivo*. Spt20 colocalized with the septin ring, but did not separate when the septin ring split. Importantly, Spt20 regulated the stability of the septin ring and was required for the recruitment of Mid2. The transcription-dependent and -independent roles of Spt20 in septin ring assembly highlight a multifaceted regulation of one process by a SAGA subunit.

KEY WORDS: SAGA, Septin, Mid2, Spt20, Fission yeast

INTRODUCTION

Cell division is a fundamental process that splits a mother cell into two daughter cells. Cell division requires the cooperation of various types of cytoskeleton, including actin filaments, intermediate filaments, microtubules and high-order septin structures. Septins are a family of GTP-binding proteins that are conserved from fungi to animals, with absences in plants (Pan et al., 2007). Septins tend to form the heterooligomeric complexes, which can be further assembled into higher-order structures, such as filaments or rings. These structures serve as a scaffold and/or diffusion barrier, and they participate in cell division and other biological processes (Mostowy and Cossart, 2012). Despite the substantial progress in the past few years, many key questions regarding the assembly of high-order septin structures remain unanswered.

[1]State Key Laboratory of Genetic Engineering, School of Life Sciences, and Institute of Biomedical Sciences, Shanghai 200433, China. [2]State Key Laboratory of Surface Physics and Department of Physics, Fudan University, Shanghai 200433, China. [3]Shanghai Engineering Research Center of Industrial Microorganisms, Shanghai 200433, China. [4]Shanghai Collaborative Innovation Center for Biomanufacturing Technology, Shanghai 200237, China.
*These authors contributed equally to this work

‡Authors for correspondence (yaoyu@fudan.edu.cn; honglu0211@yahoo.com)

Received 20 February 2014; Accepted 27 June 2014

Fission yeast, *Schizosaccharomyces pombe*, has emerged as an excellent model organism for studying septins. Seven septins have been identified so far in fission yeast. Spn1, Spn2, Spn3 and Spn4 are expressed in vegetative cells, whereas Spn5, Spn6 and Spn7 are expressed during sporulation (Onishi et al., 2010). Two copies of an Spn3–Spn4–Spn1–Spn2 complex are proposed to array in an almost linear order to form an octameric septin complex, in which Spn1 and Spn4 appear to be the core members, with Spn2 and Spn3 as auxiliary subunits (An et al., 2004). At late anaphase, the septin complex accumulates at the medial cortex of the cell, forming a primary septin ring adjacent to a contractile ring (An et al., 2004). Maturation of the septin ring requires recruitment of another protein Mid2, an anillin homolog. The periodic expression of Mid2 during the cell cycle is controlled by the Sep1–Ace2 regulatory cascade (Petit et al., 2005). In the absence of Mid2, the ring becomes unstable and diffuses as a disc at the division site (Berlin et al., 2003; Tasto et al., 2003). Shortly after the septin ring is assembled, a contractile ring starts constriction and the septum is built up in the furrow of the invaginated membrane. The septin ring does not constrict with the contractile ring and it splits into two rings as the septum develops (Berlin et al., 2003; Tasto et al., 2003). After septation, the septin ring helps to recruit hydrolytic enzymes, including Agn1 and Eng1, to cleave the septum between daughter cells (Martín-Cuadrado et al., 2005). Deletion of septin-encoding genes or *mid2*$^{+}$ causes a cell separation defect, leading to a chained cell phenotype (Berlin et al., 2003; Tasto et al., 2003; An et al., 2004). However, the mechanism underlying the assembly of a primary septin ring and the recruitment of Mid2 is still unclear.

The Spt–Ada–Gcn5–acetyltransferase (SAGA) complex is a well-known transcriptional co-activator, and is highly conserved in all eukaryotes. It is implicated in transcriptional initiation, elongation and mRNA export (García-Oliver et al., 2012). The SAGA complex can be organized into at least five modules with distinct activities. These include the histone acetyltransferase module, the histone deubiquitylation module, the TATA-binding protein (TBP)-binding module, a module for direct interaction with transcriptional activator, and a structural module (Lenstra et al., 2011; Helmlinger, 2012). The structural module consists of Spt7, Ada1 and Spt20 (Grant et al., 1997; Sterner et al., 1999). Spt20 regulates the recruitment of other subunits of SAGA and thus is required for the integrity of complex. Only a partial SAGA complex forms in an *spt20*Δ mutant in budding yeast, or in *SPT20*-knockdown HeLa cells (officially known as *SUPT20H* in humans) (Wu and Winston, 2002; Nagy et al., 2009). The biological function of Spt20 is commonly linked with the transcriptional activity of the SAGA complex. For instance, Spt20 in budding yeast is required for the transcriptional elongation of *PDR5* (Milgrom et al., 2005) and the activation of seripauperin genes upon hypoxic stress (Hickman et al., 2011). Human Spt20, also known as p38IP, participates in the regulation

Journal of Cell Science

Journal of Cell Science (2014) 127, 4024–4036 doi:10.1242/jcs.151910

of endoplasmic reticulum (ER)-stress-induced genes (Nagy et al., 2009). Nevertheless, in fission yeast, *spt20*Δ mutant cells grow much better than *spt7*Δ and *ada1*Δ mutants. *spt20*Δ cells are sensitive to 1% formamide, but *spt7*Δ and *ada1*Δ cells are not (Helmlinger et al., 2011). Different growth behaviors suggest Spt20 might act beyond the structural module.

In this study, we found that deletion of *spt20*$^{+}$ caused a severe defect in cell separation and septin ring assembly. The role of Spt20 in the septin ring assembly is partially dependent on transcriptional activation of *mid2*$^{+}$. Spt20 also regulates septin ring assembly through physical associations with Spn1–Spn4 and Mid2. Our study identifies Spt20 as a new regulator of septin ring assembly. It also provides an intriguing example of how a core subunit of a large complex can regulate a process in multifaceted ways.

RESULTS

The SAGA complex regulates cell separation independently of its enzymatic activities

In a genome-wide screen of genes involved in the DNA damage response, we previously found that *spt20*Δ cells exhibited a peak of 4C DNA content in a flow cytometry analysis (Pan et al., 2012). Duplication of DNA content could be caused by DNA re-replication, defect in cytokinesis or cell separation. To investigate the potential role of Spt20 in cell separation, we quantified the septation index of *spt20*Δ and several other SAGA mutants. Under asynchronous culture conditions, one septum was formed between wild-type (WT) daughter cells (Fig. 1A). A previous study reported that Spt8, a subunit of TBP-binding module of SAGA, is a regulator of the cell separation in fission yeast (Batta et al., 2009). As expected, 19% of *spt8*Δ cells contained two or three septa and exhibited a chained cell phenotype (Fig. 1A). Deletion of *spt20*$^{+}$ caused a slightly more severe defect in cell separation: 19% of *spt20*Δ cells contained two or three septa, 2% of cells contained more than three septa (Fig. 1A). Spt7 is regarded as the pivotal structural subunit of SAGA and *spt7*Δ mutants had the most severe defect: 35% of *spt7*Δ cells possessed two or three septa and 25% cells contained more than three septa (Fig. 1A). This suggests that Spt20, as well as the structural module and TBP-binding module of SAGA, are required for normal cell separation. In contrast, deletion of either *gcn5*$^{+}$ or *ubp8*$^{+}$ did not cause any cell separation defect (Fig. 1A). Given that the histone acetylation and deubiquitylation activities of the SAGA complex are rendered by Gcn5 and Ubp8 (García-Oliver et al., 2012), these results suggest that SAGA complex regulates cell separation independent of its enzymatic activities.

Flow cytometry analysis was performed to confirm the cell separation defect of SAGA mutants (Fig. 1B). WT cells exhibited a distinct peak equivalent to 2C DNA content, the same as *upb8*Δ cells. A *gcn5*Δ mutant contained peaks at 1C and 2C DNA content, suggesting a possible delay in G1 phase (Espinosa et al., 2010). Consistent with the results of septation index analysis, *spt8*Δ, *spt20*Δ or *spt7*Δ mutants contained peaks around 4C and 8C DNA content, indicating a defect in cell separation.

The role of Spt20 or Spt7 in the cell separation is not completely mediated by transcriptional activation of *ace2*$^{+}$

Deletion of *spt8*$^{+}$ causes a cell separation defect by reducing the levels of *ace2*$^{+}$ and its target genes (Batta et al., 2009). Ace2 is a master transcription activator that controls most of the cell separation genes, including *agn1*$^{+}$, *eng1*$^{+}$ and *mid2*$^{+}$ (Alonso-Nuñez et al., 2005). Given that *spt20*Δ and *spt7*Δ mutants displayed a defect in cell separation, we analyzed the levels of *ace2*$^{+}$, *agn1*$^{+}$, *eng1*$^{+}$ and *mid2*$^{+}$ in these mutants. mRNA levels of *ace2*$^{+}$ and three Ace2-targeted genes all decreased in *spt20*Δ and *spt7*Δ mutants, as well as in an *spt8*Δ mutant (Fig. 2A). The data are consistent with a previous microarray analysis (Helmlinger et al., 2011). Hence, Spt20 and Spt7 are required for the

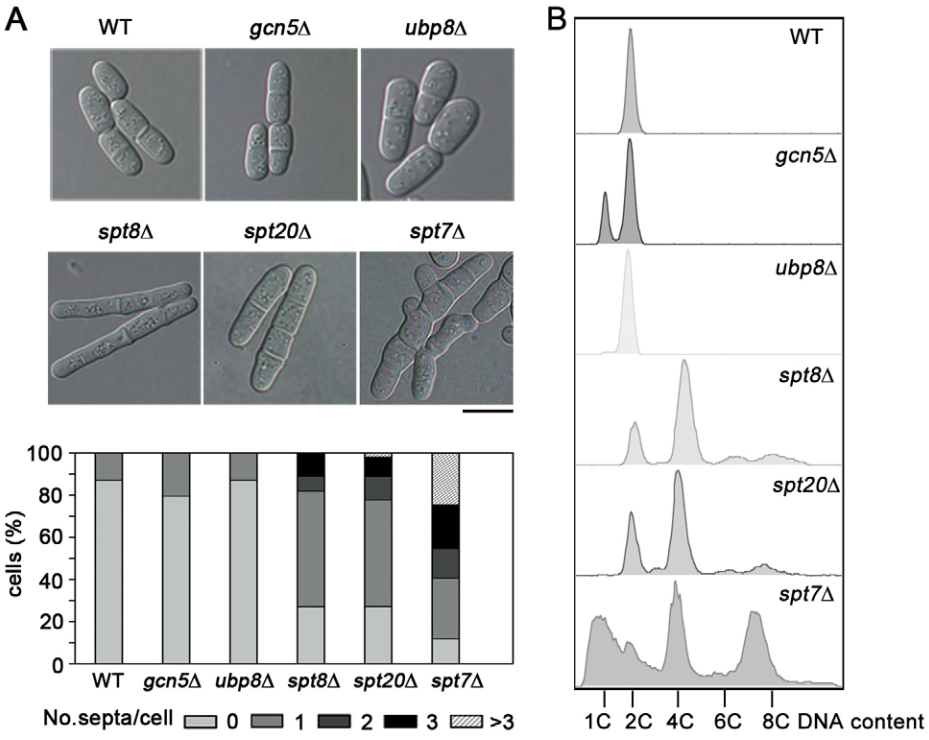

Fig. 1. The SAGA complex regulates cell separation independently of its enzymatic activities. (A) Septation indexes of representative SAGA mutants. WT (LHP164), *gcn5*Δ (LHP165), *ubp8*Δ (LHP166), *spt8*Δ (LHP167), *spt20*Δ (LHP168) or *spt7*Δ (LHP169) cells were grown in YES medium and collected during the exponential phase. Representative differential interference contrast (DIC) images of cells are shown at the top, and the proportion of cells with different numbers of septa are shown at the bottom. More than 400 cells were counted in each sample. Scale bar: 10 μm. (B) Flow cytometry analysis of the cells shown in A to analyze their DNA content.

Journal of Cell Science (2014) 127, 4024–4036 doi:10.1242/jcs.151910

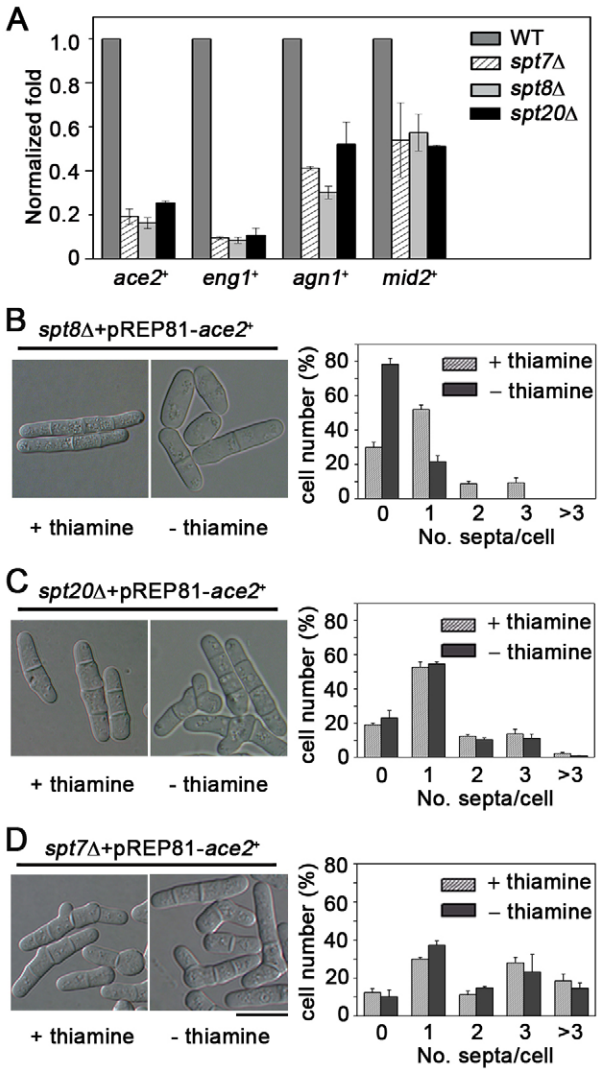

Fig. 2. The cell separation defect of *spt20*Δ or *spt7*Δ cannot rescued by enhanced expression of *ace2*$^+$. (A) Quantitative analysis of mRNA levels of *ace2*$^+$, *eng1*$^+$, *agn1*$^+$ and *mid2*$^+$ in wild-type (LHP164), *spt20*Δ (LHP168), *spt8*Δ (LHP167) or *spt7*Δ (LHP169) cells. Cells were grown in YES medium and collected during the exponential phase. RNA was extracted and reverse-transcribed into cDNA for quantitative PCR. The level of *act1*$^+$ was used for normalization. The mRNA level in WT cells was designated as 1 for comparison. Each column represents the mean±s.d. (n=3). (B–D) Effect of enhanced expression of *ace2*$^+$ in *spt8*Δ (B), *spt20*Δ (C) and *spt7*Δ (D) cells. Cells were transformed with pREP81-*ace2*$^+$. Transformants were grown in EMM2 without leucine and were collected during exponential growth. Expression of *ace2*$^+$ was driven by an *nmt81*$^+$ promoter, which is repressed in the medium supplemented with 15 μM thiamine (+ thiamine), and is induced in the medium without thiamine (–thiamine). Representative DIC images of cells are shown on the left and the proportion of cells with different numbers of septa are shown on the right. More than 200 cells were counted in one independent experiment for each sample. Each column represents the mean±s.d. (n=3). Scale bar: 10 μm.

transcriptional activation of *ace2*$^+$. However, whether such activation could completely account for the effects of Spt20 or Spt7 on cell separation was unknown. To address this question, we increased the level of *ace2*$^+$ in WT and mutant cells. As reported previously (Batta et al., 2009), enhanced expression of *ace2*$^+$ eliminated the multiple-septa cells in *spt8*Δ mutants and thus fully restored normal cell separation (Fig. 2B). In contrast, no significant improvement was observed in the *spt20*Δ or *spt7*Δ cells with elevated level of *ace2*$^+$ (Fig. 2C,D). Therefore, the contribution of Spt20 or Spt7 to the cell separation is not limited to transcriptional activation of *ace2*$^+$.

The SAGA complex is required for the septin ring assembly

Abnormal septin ring assembly leads to a severe cell separation defect (Sipiczki, 2007). Given that the expression of *mid2*$^+$, which encodes a factor required for the stability of the septin ring, was reduced by half in *spt7*Δ, *spt8*Δ and *spt20*Δ cells, we investigated whether septin ring assembly was impaired in these mutants. We tagged endogenous Spn1 with GFP and observed its fluorescent signal at the division sites in WT and mutant cells. Because the septin ring dissipates after cell separation (Berlin et al., 2003; Tasto et al., 2003), the septin signal tends to be lost at an un-cleaved septum in a multiple-septa cell. To avoid overestimation of signal loss, multiple-septa cells were excluded for the quantitation. Cells with a visible septum, and with a length shorter than 15 μm, were included for analysis. 100% of WT cells contained a septin signal at the division site, which was seen as a distinct ring structure (Fig. 3). Approximately 30% of *mid2*Δ cells lost septin signals at the division sites, consistent with the role of Mid2 in maintaining a stable septin ring structure (Fig. 3) (Berlin et al., 2003; Tasto et al., 2003). In *spt7*Δ or *spt8*Δ mutants, ~30% of cells lost septin signals at the division sites (Fig. 3). These observations suggest that the TBP-binding module and the structural module of the SAGA complex contribute to septin ring assembly. As expected, the septin ring assembly was not affected in *gcn5*Δ and *ubp8*Δ mutants, consistent with normal cell separation in both mutants (Fig. 3). Thus, the enzymatic activity of the SAGA complex is dispensable for septin ring assembly.

In the case of the *spt20*Δ mutant, ~80% of cells lost septin signals at the division sites. Meanwhile, septins were ectopically localized at cell tips or in the cytoplasm of *spt20*Δ cells, similar to the localization of septin dots during interphase (Fig. 3) (Berlin et al., 2003; Tasto et al., 2003). Importantly, the assembly defect of *spt20*Δ cells (80% loss) was much more severe than that of *mid2*Δ cells (30% loss). Therefore, other transcriptional targets besides Mid2, especially the ones under the control of Ace2, might contribute to the phenotype of *spt20*Δ cells. It was also possible that Spt20 regulates septin ring assembly in a transcription-independent way, which was then investigated.

Spt20 is associated with the components of the septin ring *in vitro* and *in vivo*

A mature septin ring is composed of Spn1, Spn2, Spn3, Spn4 and Mid2. We investigated whether Spt20 regulates the level of other components of the septin ring besides Mid2. As expected, the level of Mid2 protein was reduced by 26% in *spt20*Δ cells (Fig. 4A). However, protein levels of all four septins in *spt20*Δ cells were the same as those in WT cells (Fig. 4A). Therefore, Spt20 regulates septin ring assembly without affecting the levels of septins.

We next asked whether Spt20 interacts with components of the septin ring directly. As shown in Fig. 4B, Spn2 or Mid2 expressed by an *in vitro* translation system could be pulled down by immobilized GST–Spt20, but not by GST alone. The results indicate that Spt20 interacts directly with Spn2 and Mid2 *in vitro*. In another pulldown assay, GST–Spt20, but not GST, could bind to Spt20–His$_6$, suggesting that Spt20 interacts with itself (Fig. 4B). To investigate the associations *in vivo*, we conducted co-immunoprecipitation (Co-IP) assays in the cells

Journal of Cell Science (2014) 127, 4024–4036 doi:10.1242/jcs.151910

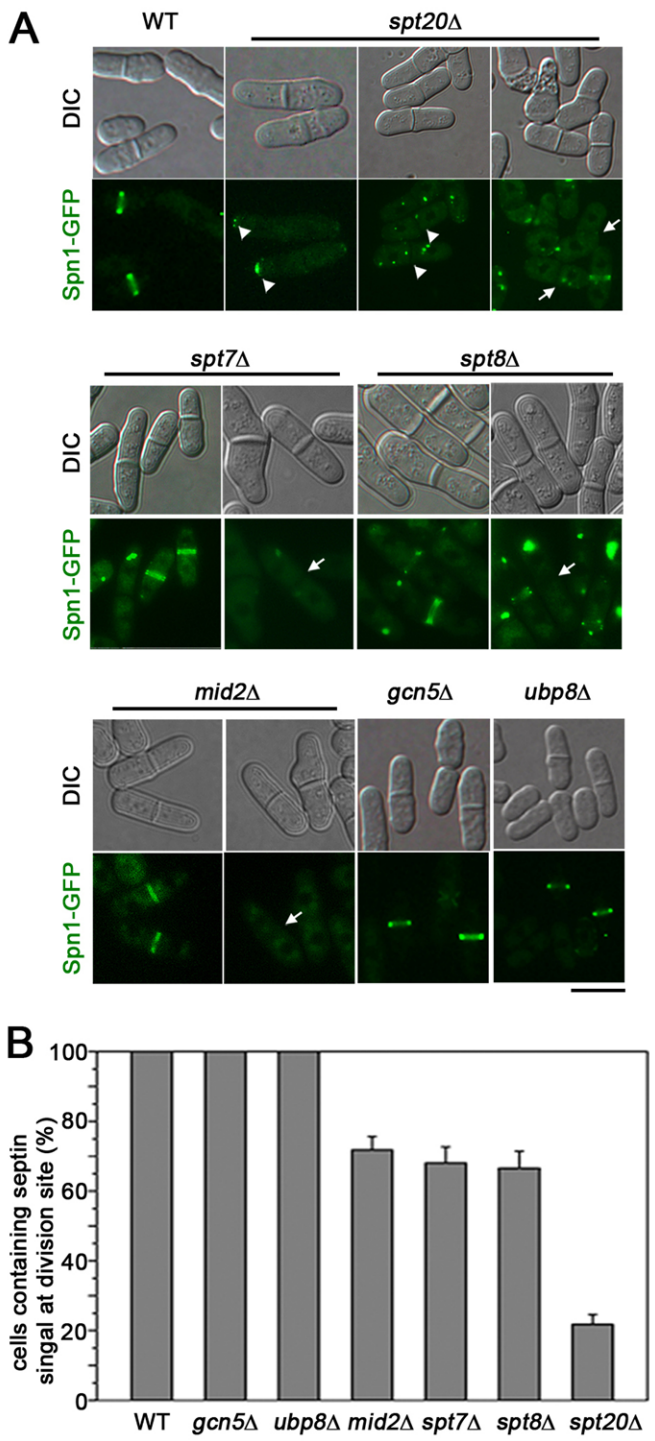

Fig. 3. Spt20 is required for septin ring assembly at a division site. (A) WT (LHP44), *spt20*Δ (LHP124), *spt7*Δ (LHP128) *spt8*Δ (LHP129), *gcn5*Δ (LHP126), *ubp8*Δ (LHP127), or *mid2*Δ (LHP148) cells expressing Spn1–GFP were collected during exponential growth. Representative DIC and GFP (green) fluorescence images of living cells are shown. In *spt20*Δ cells, ectopic localizations of Spn1–GFP at cell ends or in the cytoplasm are indicated by arrowheads. In *spt20*Δ, *spt7*Δ, *spt8*Δ or *mid2*Δ mutants, cells that lost septin signal at the division site are indicated by arrows. Scale bar: 10 μm. (B) The proportion of cells containing a septin signal at the division site is shown. Cell with a visible septum and a length shorter than 15 μm were counted. More than 200 cells were counted in one independent experiment for each sample. Each column represents the mean±s.d. (n=3).

overexpressing HA-tagged Spt20 and FLAG-tagged components of the septin ring. Spt20–HA could be detected in the anti-FLAG immunoprecipitates from the lysates of cells expressing FLAG–Spn1, FLAG–Spn2, FLAG–Spn3, FLAG–Spn4 or FLAG–Mid2, but not from lysate of cells expressing FLAG tag alone (Fig. 4C–G). These results suggest that Spt20 is associated with the components of the septin ring *in vivo*.

Spt20 colocalizes with septin rings at the division sites

Given that Spt20 associated with the subunits of the septin ring *in vivo*, we speculated that Spt20 should colocalize with the septin ring at the division site. Endogenous Spt20 was tagged with triple mCherry ($mCherry_3$) and Spn4 with GFP for visualization of the septin ring. As described previously (Matsuyama et al., 2006), Spt20–$mCherry_3$ was localized predominantly in the nucleus, probably within the SAGA complex (Fig. 5A). Although Spn4–GFP appeared at the division site as a discrete ring structure, Spt20–$mCherry_3$ colocalized with Spn4–GFP in 50% of cells (n=150). However, 50% of the cells contained a signal for Spn4–GFP but not for Spt20–$mCherry_3$ at the division site. No cells were found to harbor Spt20–$mCherry_3$ at a division site in the absence of Spn4–GFP (n>200). Therefore, localization of Spn4 at the division site might precede that of Spt20. The septin ring splits into two rings which sandwich the newly formed septum (Berlin et al., 2003; Tasto et al., 2003). It is interesting that the Spt20–$mCherry_3$ did not separate, whereas Spn4–GFP split into double rings. As a consequence, Spt20–$mCherry_3$ resided between the Spn4–GFP (Fig. 5A). This suggests that Spt20 dissociates from the septin ring before the septum forms.

The colocalization of Spt20–$mCherry_3$ and Spn4–GFP was confirmed by fluorescence resonance energy transfer (FRET) analysis. After excitation of the GFP fluorophore, increased emission in the mCherry channel in the middle of cell revealed FRET (Fig. 5B). The close proximity required for the occurrence of FRET (R_0=5 nm) suggests that Spn4–GFP interacts with Spt20–$mCherry_3$ directly. In some other cells, excitation of GFP led to the emission in the GFP channel but not in the mCherry channel (Fig. 5B). This result suggests that Spt20–$mCherry_3$ is absent at the division site of these cells, which is consistent with the idea that Spn4 might be localized to the septin ring ahead of Spt20. As a control, the excitation of GFP in cells expressing Spn4–GFP alone did not produce FRET, excluding the interference of autofluorescence (Fig. 5B).

The data shown above suggest the medial localization of Spn4 precedes that of Spt20. We therefore examined whether the localization of Spt20 was dependent on the formation of a septin ring. As shown in Fig. 5C, the signals of Spn4–GFP at the division sites were missing in the *spn1*Δ cells, indicating that the septin ring structures were abolished. Meanwhile, the medial localization of Spt20–$mCherry_3$ was totally lost (n>150), suggesting that the assembly of a septin ring is required for the recruitment of Spt20.

Overexpressing Spt20 causes a severe septin ring assembly defect in *spn2*Δ cells

As shown in Fig. 4B, Spt20 interacts with Spn2 and Mid2 directly. The interdependence of the three proteins in ring assembly was investigated by a genetic analysis. Consistent with a previous study (An et al., 2004), the defect of septin ring assembly in *spn2*Δ cells was very mild, suggesting that Spn2 is an auxiliary subunit of the ring (Fig. 6A). 30% of *mid2*Δ cells lost septin signals at the division sites. Combination of the deletion of

Journal of Cell Science (2014) 127, 4024–4036 doi:10.1242/jcs.151910

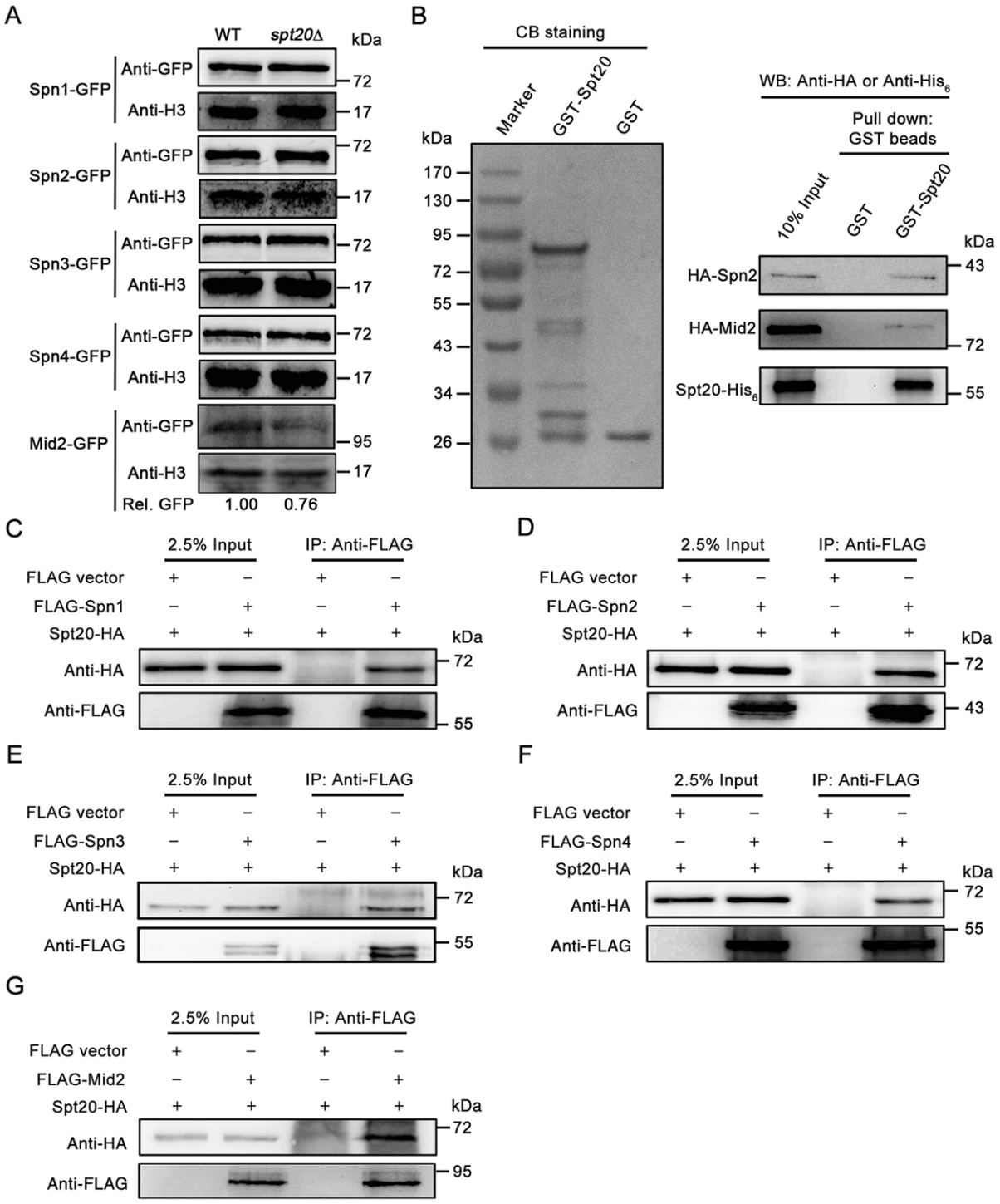

Fig. 4. Spt20 is associated with components of septin ring *in vitro* and *in vivo*. (A) Protein levels of septins and Mid2 in WT or *spt20*Δ cells. Relevant strains include: WT cells expressing Spn1–GFP (LHP44), Spn2–GFP (FY14936), Spn3–GFP (FY14998), Spn4–GFP (LHP45) or Mid2–GFP (LHP133); *spt20*Δ cells expressing Spn1–GFP (LHP124), Spn2–GFP (LHP131), Spn3–GFP (LHP132), Spn4–GFP (LHP130) or Mid2–GFP (LHP134). Cells were collected during exponential growth. Whole-cell extract was prepared and western blotting (WB) was performed using anti-GFP and anti-histone H3 antibody. The relative level of GFP (Rel. GFP) was calculated by quantifying the relative density of Mid2–GFP against H3. (B) Results of a pulldown assay to detect the interactions between Spt20 and the components of the septin ring. GST or GST–Spt20 was immobilized on GST beads and was mixed with an *in vitro* translation product containing HA-tagged Spn2 or Mid2. In another assay, immobilized GST or GST–Spt20 was mixed with Spt20–His_6 purified by the pET system. After the beads were thoroughly washed, proteins conjugated to the beads were detected by western blotting using anti-HA or anti-His_6 antibody. Coomassie blue (CB) staining of the GST proteins for pulldown assay is shown on the left. (C–G) Results of a co-immunoprecipitation assay to detect the association between Spt20 and the components of the septin ring. Cells (LHP164) were co-transformed a plasmid expressing HA-tagged Spt20 (pJR2-41U-Spt20-HA) and a plasmid expressing FLAG-tagged Spn1 (C), Spn2 (D), Spn3 (E), Spn4 (F) or Mid2 (G). As control, cells were co-transformed pJR2-41U-Spt20-HA and vector expressing FLAG tag alone. The transformants were grown in EMM2 medium without leucine and uracil and collected during exponential growth. Spt20 in the anti-FLAG immunoprecipitate was detected by western blotting using anti-HA antibody. The input is shown on the left and immunoprecipitated (IP) proteins on the right.

Journal of Cell Science (2014) 127, 4024–4036 doi:10.1242/jcs.151910

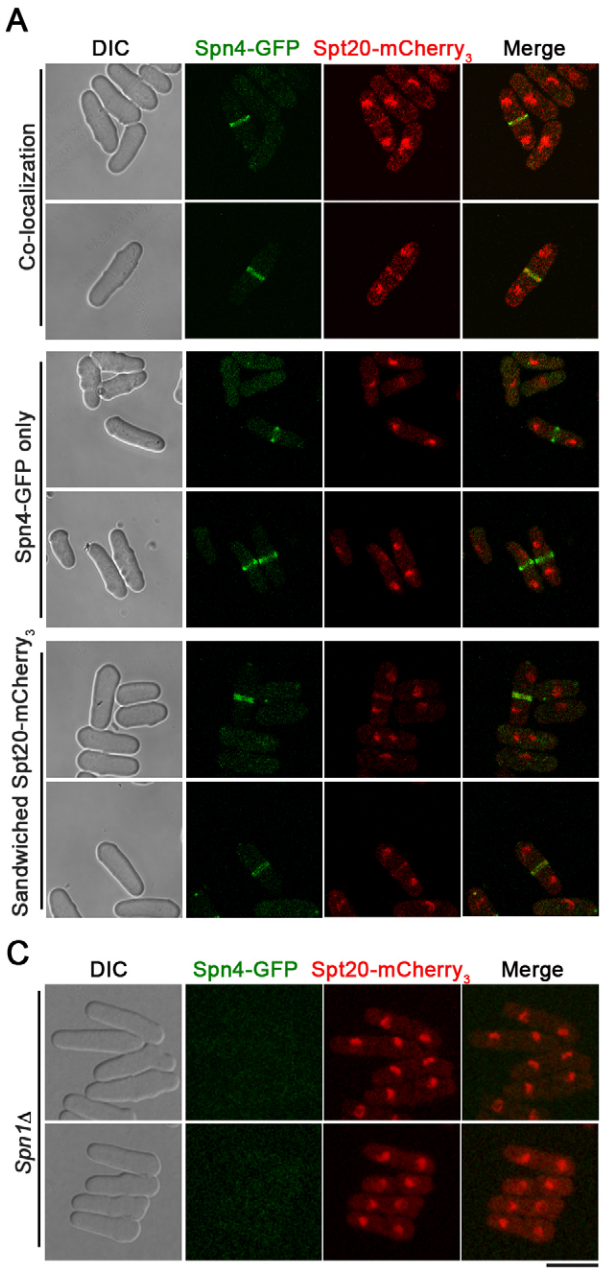

Fig. 5. Spt20 colocalizes with the septin ring *in vivo*. (A) Localizations of Spn4–GFP and Spt20–mCherry$_3$. WT (LHP135) cells co-expressing Spn4–GFP and Spt20–mCherry$_3$ were collected during exponential growth. Cells were fixed in 100% ethanol before imaging. Representative DIC, mCherry (red) and GFP (green) fluorescence images are shown. Top, Spt20–mCherry$_3$ colocalized with Spn4–GFP at the division site. Middle, cells contained the Spn4–GFP signal but not that of Spt20–mCherry$_3$ at the division sites. Bottom, when the Spn4–GFP signal splits, the Spt20 signal is present between that of Spn4–GFP. (B) FRET analysis of the interaction between Spn4–GFP and Spt20–mCherry$_3$. Cells were collected and fixed as described in A. Selected frames of videos are shown. Top, excitation of GFP led to the emission in the mCherry channel in the middle of WT cells (LHP135). Middle, excitation of GFP in WT cells led to the emission in the GFP but not in the mCherry channel. Bottom, excitation of GFP in cells expressing Spn4–GFP (LHP45). (C) Localizations of Spn4–GFP and Spt20–mCherry$_3$ in *spn1*Δ cells. LHP174 were collected and fixed as described in A. Representative DIC mCherry (red) and GFP (green) fluorescence images are shown. Scale bar: 10 μm.

mid2$^+$ or *spn2*$^+$ with deletion of *spt20*$^+$ exhibited the same extent of the assembly defect as single deletion of *spt20*$^+$ (Fig. 6A). These results indicate that Spt20, Mid2 and Spn2 act in the same pathway.

The relationship between Spn2 and Spt20 was further investigated in a functional complementation test. Overexpressing *spn2*$^+$ could not rescue the defect of ring assembly or cell separation in *spt20*Δ cells (Fig. 6B,C). In contrast, overexpressing *spt20*$^+$ substantially exaggerated the ring assembly defect in *spn2*Δ cells, leading to a 50% drop in the number of cells containing a septin signal at the division sites. Meanwhile, overexpressing Spt20 increased the amount of ectopic septin structures in the cytoplasm (Fig. 6D) and exacerbated the cell separation defect of *spn2*Δ mutant (Fig. 6E). The result suggests that in the absence of Spn2, a compromised septin ring tends to collapse in the presence of an excess amount of Spt20. Accordingly, it is known that overexpressing a septin-associated regulator might interfere with the higher-ordered septin structures *in vivo* (Qiu et al., 2008; Kang et al., 2013).

To validate whether the impact of overexpressing *spt20*$^+$ was specific to *spn2*Δ cells, we overexpressed *spt20*$^+$ in WT cells. Overproduction caused a ~10% drop in the number of cells with a medial Spn1–GFP signal and slightly increased the number of multiple-septa cells (Fig. 6F,G). This relatively small defect might be related to the general roles of SAGA in septin ring assembly, because overexpressing *spt7*$^+$ in *spn2*Δ or WT cells also caused a ~10% drop in the number of cells with a Spn1–GFP signal at the division site and led to a mild separation defect (Fig. 6H–K). In comparison, the assembly defect was much more severe in the combination of overproduction of *spt20*$^+$ and the deletion of *spn2*$^+$ (Fig. 6D), suggesting a specific functional relationship between Spt20 and Spn2.

Journal of Cell Science (2014) 127, 4024–4036 doi:10.1242/jcs.151910

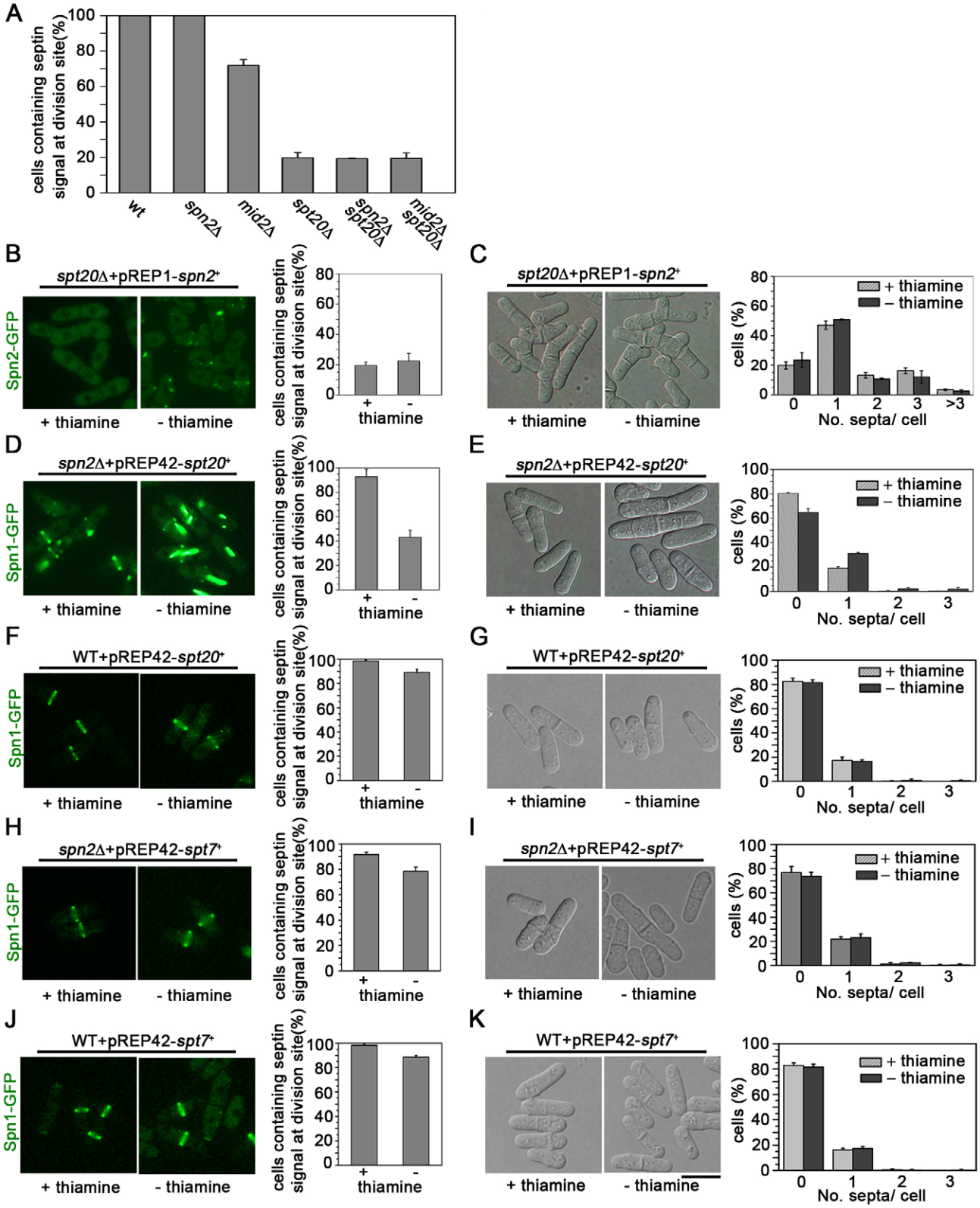

Fig. 6. See next page for legend.

Spt20 is required for the recruitment of Mid2

The interaction between Spn2 and Mid2 hints at a potential role for Spt20 in the recruitment of Mid2 onto the septin ring. To test this possibility, we tagged endogenous Mid2 with mCherry and examined its colocalization with Spn1–GFP in WT and *spt20*Δ cells. Among the cells with Spn1–GFP signal present at the division site, 66% of WT cells contained colocalized Mid2–mCherry signal, whereas only 6% of *spt20*Δ cells contained

Journal of Cell Science (2014) 127, 4024–4036 doi:10.1242/jcs.151910

Fig. 6. Overexpressing Spt20 caused a severe defect of septin ring assembly in *spn2*Δ cells. (A) Septin ring in the *spt20*Δ mutant combined with deletion of *mid2*$^+$ or *spn2*$^+$. WT (LHP44), *spn2*Δ (LHP150), *mid2*Δ (LHP148), *spt20*Δ (LHP124), *spn2*Δ *spt20*Δ (LHP141), and *mid2*Δ *spt20*Δ (LHP139) cells expressing Spn1–GFP were collected during exponential growth. Cells mentioned below were also collected during exponential growth. The proportion of cells containing septin signal at the division site was quantified. Cells with a visible septum and a length shorter than 15 μm was counted in A and below (>200 cells in one independent experiment for each sample). Each column shown in A and below represents the mean±s.d. (n=3). (B–K) Results of the functional complementation experiments. *spt20*Δ cells (LHP131) were transformed with pREP1-*spn2*$^+$ (B,C), *spn2*Δ cells (LHP150) with pREP42-*spt20*$^+$ (D,E), WT cells (LHP44) with pREP42-*spt20*$^+$ (F,G), *spn2*Δ cells with pREP42-*spt7*$^+$ (H,I), and WT cells with pREP42-*spt7*$^+$ (J,K). Transformants were grown in EMM2 medium without leucine or in EMM2 medium without uracil. Expression of *spt20*$^+$, *spn2*$^+$ or *spt7*$^+$ on the plasmid was repressed in the medium supplemented with 15 μM thiamine (+ thiamine) and was induced in the medium without thiamine (–thiamine). Septin signals at the division sites were visualized by Spn2–GFP in B, or by Spn1–GFP in D, F, H and J. In B, D, F, H and J, the proportion of cells containing septin signal at the division site are shown on the right and representative GFP fluorescence images on the left. In C, E, G, I and K, the proportion of cells with different numbers of septa are shown on the right and representative DIC images on the left. Scale bar: 10 μm.

colocalized Mid2–mCherry (Fig. 7A). Accordingly, the septin in *spt20*Δ cells did not assemble as a ring but showed a diffuse disc localization across the septum. This phenotype resembled the situation in *mid2*Δ cells (Fig. 7B). As controls, WT and *spn2*Δ cells contained distinct septin rings at their division sites (Fig. 7B). The severe defect of Mid2 recruitment might not be explained solely by the reduced level of Mid2 in the *spt20*Δ mutant, because deletion of *spt20*$^+$ only caused a 26% reduction of protein level of Mid2 (Fig. 4A). It is likely that Spt20 contributes to the recruitment of Mid2, not only through the transcriptional activation of *mid2*$^+$, but also through the interaction between Spt20 and Mid2.

A functional complementation test was performed to further investigate the relationship between Spt20 and Mid2. Overexpressing *mid2*$^+$ significantly restored the septin signals at the division sites of *spt20*Δ cells (Fig. 7C). The rescue might be achieved in the multiple ways. First, overexpression of *mid2*$^+$ was able to compensate for the reduced transcriptional level of *mid2*$^+$ in *spt20*Δ cells. Second, overexpressing *mid2*$^+$ might bypass the requirement of Spt20–Mid2 interaction for the recruitment of Mid2. Third, the increased level of Mid2 might stabilize the compromised septin structure in the absence of Spt20. As shown in Fig. 7D, overexpressing *mid2*$^+$ also substantially rescued the cell separation defect of *spt20*Δ cells. This suggests that the cell separation defect in *spt20*Δ cells is mainly due to a defective septin ring assembly. In a reciprocal assay, overexpressing *spt20*$^+$ could not rescue the defects of septin ring assembly and cell separation in *mid2*Δ cells, which is consistent with the idea that Spt20 acts upstream of Mid2 in ring assembly (Fig. 7E,F).

Given that the mRNA levels of *mid2*$^+$ decreased in *spt7*Δ and *spt8*Δ mutants (Fig. 2A), a functional complementation test was also performed in these two mutants. However, overexpressing *mid2*$^+$ in *spt7*Δ or *spt8*Δ cells could neither increase the medial signal of Spn1–GFP nor rescue the cell separation defect (Fig. 7G–J), suggesting that the defects in *spt7*Δ or *spt8*Δ mutant are not primarily due to a reduced transcriptional level of *mid2*$^+$. Hence, the roles of Spt7 and Spt8 in septin ring assembly and cell separation are probably different from that of Spt20.

Spt20 and Spn2 bind with Mid2 in a competitive manner

Previous studies have indicated that Spn2 forms a primary septin ring with Spn1, Spn3 and Spn4 at the medial region. Slightly later, Mid2 is recruited to the structure to form a stable septin ring (Berlin et al., 2003; Tasto et al., 2003; An et al., 2004). Given that Spt20 is able to interact with Spn2 and Mid2, which are present at different stages of septin ring assembly, we investigated the interactions among these three proteins. In a pulldown assay, immobilized GST–Mid2 could pulldown Spt20–His_6 and Spn2–His_6 (Fig. 8A). Notably, with the increased amounts of Spt20–His_6, the level of Mid2-bound Spn2–His_6 decreased gradually. In a control assay, the level of Mid2-bound Spn2–His_6 was not affected by the amount of pullulanase-His_6 (Pul–His_6), which is not associated to Spt20 or septins (Fig. 8B). These results imply that Spt20 and Spn2 bind with Mid2 in a competitive manner.

DISCUSSION

The role of SAGA subunits in cell separation

As shown in Fig. 1, the histone acetylation and deubiquitylation activity of the SAGA complex is dispensable for cell separation. By contrast, *spt8*Δ cells showed a defect in cell separation, suggesting that the TBP-binding module is required for normal cell separation. Accordingly, deletion of Spt3, another subunit of the TBP-binding module, also leads to a severe chain phenotype (Y.Y., unpublished data). Given that a modest overexpression of *ace2*$^+$ could fully rescue the cell separation defect of *spt8*Δ cells, the TBP-binding module might regulate cell separation mostly through transcriptional activation of *ace2*$^+$, which could be achieved by the recruitment of TBP to the promoter of *ace2*$^+$. A similar case, the histone-acetyltransferase-independent activation of *GAL1* by Spt3, has been reported in budding yeast (Yu et al., 2003).

Spt20 and Spt7 are required for the integrity of the SAGA complex (Sterner et al., 1999). Deletion of either subunit will undermine the function of the other modules, including the TBP-binding module. The expression levels of *ace2*$^+$ and three Ace2-targeted genes in *spt20*Δ and *spt7*Δ mutants were similar to those in *spt8*Δ mutant (Fig. 2A). Therefore, Spt7 and Spt20 might regulate transcriptional activation of *ace2*$^+$ through the TBP-binding module. But the contribution of Spt7 and Spt20 to cell separation is not exclusively mediated by the activation of *ace2*$^+$ (Fig. 2B). As shown in this study, Spt20 plays a transcription-independent role in the septin ring assembly. Spt7 is regarded as one of the pivotal structural subunits of the SAGA complex. Deletion of Spt7 causes the dissociation of most modules and thus abolishes the activity of SAGA complex (Wu and Winston, 2002). According to a comprehensive transcriptome analysis of SAGA mutants (Helmlinger et al., 2011), the level of *gar2*$^+$, whose deletion causes a chain phenotype (Gulli et al., 1997), was substantially downregulated in a *spt7*Δ mutant but not in a *spt8*Δ and *spt20*Δ mutant. Whether Spt7 regulates cell separation through the transcriptional activation of *gar2*$^+$ and other genes remains to be determined.

Spt20 is a regulator of septin ring assembly

Spt20 is required for the transcriptional activation of *mid2*$^+$, which is probably an indirect outcome of activation of *ace2*$^+$ (Fig. 2A). The regulation reflects a transcription-dependent role of Spt20 in the septin ring assembly, which probably relies on the activity of the SAGA complex. It is surprising to uncover a transcription-independent role of Spt20 in septin ring assembly.

Journal of Cell Science (2014) 127, 4024–4036 doi:10.1242/jcs.151910

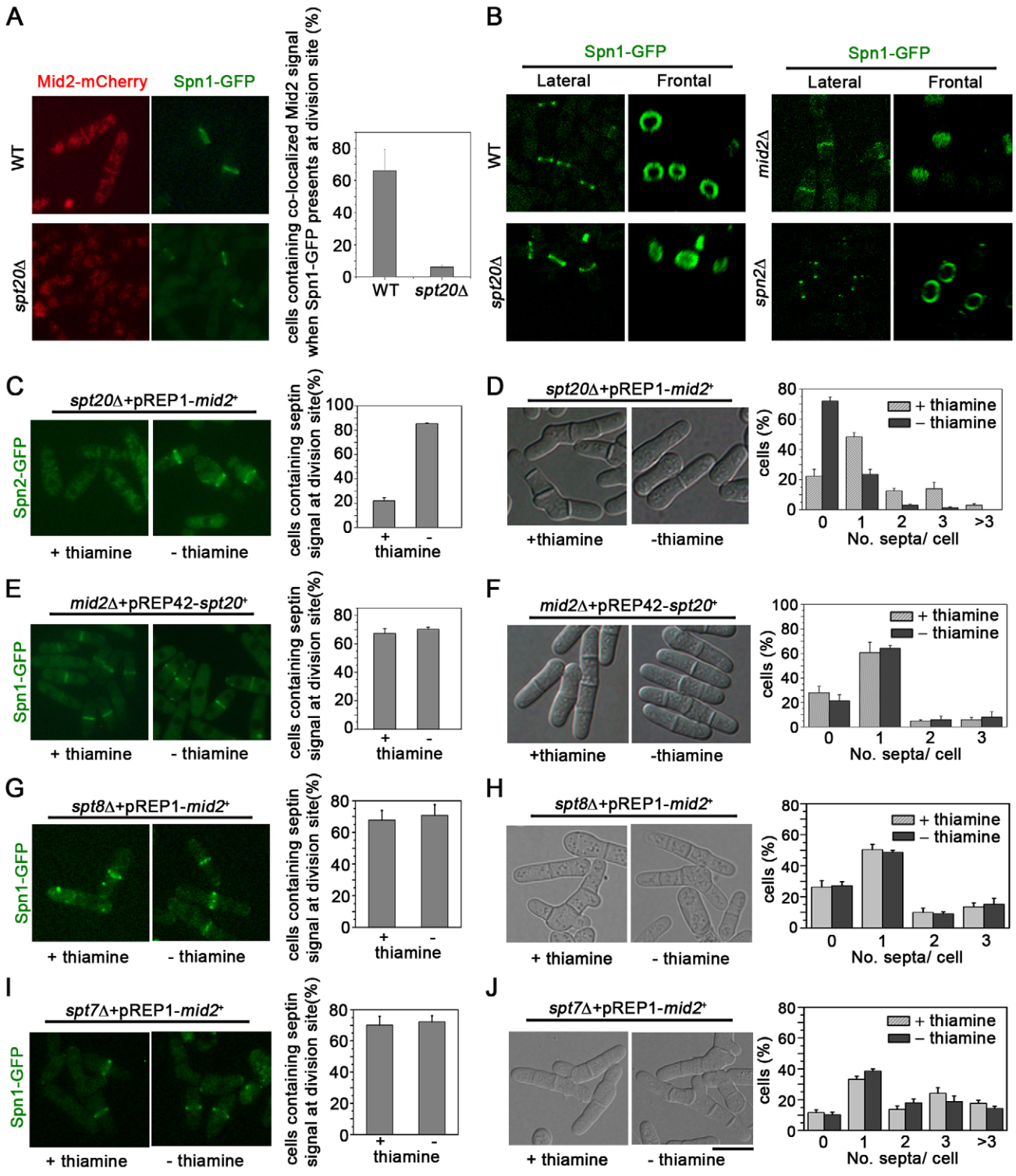

Fig. 7. See next page for legend.

Spt20 interacts directly with Spn2 and Mid2 *in vitro* and is associated with other components of the septin ring *in vivo* (Fig. 4). In addition, Spt20 colocalized with the septin ring at the division sites (Fig. 5). In the past decade, it has become apparent that septin-associated regulators contribute substantially to the organization of high-order septin structures. Some well-studied regulators include Anillin/Mid2, Bogr3, Bni5 and Syp1 (Oegema et al., 2000; Joberty et al., 2001; Lee et al., 2002; Berlin et al., 2003; Tasto et al., 2003; Qiu et al., 2008). Our study suggests Spt20 is a new member of this growing list.

As shown in Fig. 5A, the localization of Spn4 at the division site preceded that of Spt20. Given that Spn4 is an indispensable subunit of a primary septin ring (An et al., 2004), this suggests that the primary septin ring is assembled before the recruitment of

Fig. 7. Spt20 is required for the recruitment of Mid2. (A) Mid2–mCherry signal in WT (LHP163) and *spt20*Δ (LHP162) cells. Representative fluorescence images of living cells are shown on the left. The proportion of cells that contain colocalized Mid2–mCherry when Spn1–GFP is present at the division site is shown on the right. More than 100 cells were counted in one independent experiment for each sample. Each column shown in A and below represents the mean±s.d. (n=3). (B) Frontal and lateral views of septin ring in WT (LHP44), *spt20*Δ (LHP124), *mid2*Δ (LHP148) and *spn2*Δ (LHP150) cells. Cells with medial septin signals were selected for representation and Spn1–GFP was visualized using confocal three-dimensional microscopy. (C–J) Results of the functional complementation experiments. *spt20*Δ cells (LHP131) were transformed with pREP1-*mid2*$^+$ (C,D), *mid2*Δ cells (LHP148) with pREP42-*spt20*$^+$ (E,F), *spt8*Δ cells (LHP129) with pREP1-*mid2*$^+$ (G,H), and *spt7*Δ cells (LHP128) with pREP1-*mid2*$^+$ (I,J). Transformants were grown in EMM2 medium without leucine or in EMM2 medium without uracil, and were collected during the exponential phase. Expression of *spt20*$^+$ or *mid2*$^+$ on the plasmid was repressed in the medium supplemented with 15 μM thiamine (+ thiamine) and induced in the medium without thiamine (– thiamine). Septin signals at the division sites were visualized by Spn2–GFP in C, or by Spn1–GFP in E, G and I. In C, E, G and I, the proportion of cells containing a septin signal at the division site are shown on the right and representative GFP fluorescence images on the left. Cell with a visible septum and a length shorter than 15 μm were counted. In D, F, H and J, the proportion of cells with different numbers of septa are shown on the right and representative DIC images on the left. More than 200 cells were counted in one independent experiment of each sample in C–J. Scale bar: 10 μm.

Spt20. Accordingly, deletion of Spn1, another indispensable subunit of a primary septin ring, abolished the medial localization of Spt20 (Fig. 5C). It is unclear how Spt20 is recruited to the primary septin ring. Because Spt20 interacts with Spn2 directly *in vitro*, Spn2 might contribute to the recruitment of Spt20 (Fig. 3B). However, the recruitment is not dependent solely on Spn2, as the defect of septin ring assembly in *spn2*Δ cells was much milder than that in *spt20*Δ cells (Fig. 6A). Other components of the primary septin ring might be involved in the recruitment of Spt20. After the recruitment, Spt20 might regulate the stability of the primary septin ring, because loss of septin ring in *spt20*Δ cells (80% loss) is more severe than that in *mid2*Δ cells (30% loss) (Fig. 3B). Meanwhile, the amount of Spt20 must be fine-tuned, because overexpressing Spt20 caused a severe defect of septin ring assembly in *spn2*Δ cells (Fig. 6D).

Another important role of Spt20 in the septin ring assembly is reflected by the multilayered crosstalk between Spt20 and Mid2. First, Spt20 is required for the transcriptional activation of *mid2*$^+$. Second, Spt20 interacts with Mid2 directly and that interaction might contribute to the recruitment of Mid2 onto the ring. In the absence of Spt20, the signal of Mid2 on the septin ring was almost totally lost and the ring became unstable and diffusive (Fig. 6A,B). In one attractive model, Mid2 is associated with Spt20 in the cytoplasm, and then the Mid2–Spt20 pair might be targeted to the ring through Spt20–Spt20 interaction (Fig. 4B). Third, Spt20 and Spn2 bind with Mid2 in a competitive manner *in vitro*. This suggests that the recruitment of Mid2 might cause competition between Spt20 and Spn2. The competition might lead to the dissociation of Spt20 from the ring. The dissociation becomes observable during cell septation, when Spt20 is sandwiched between the separated septin rings (Fig. 5A).

Transcription-independent functions of SAGA subunits

Intriguingly, the transcription-independent role of Spt20 is not an exceptional case seen only in fission yeast. In mammals, a homolog of Spt20 was first identified as a binding partner of p38 mitogen-activated protein kinase (MAPK14) and so is known as p38IP. p38IP and p38 MAPK are required for downregulation of E-cadherin, a transmembrane protein. Notably, the regulation takes place at the post-transcriptional level, distinct from regulation by the SAGA complex (Zohn et al., 2006). In another study, p38IP has been shown to interact with mammalian (m)Atg9 (ATG9A) on the endosomal membrane. In the rich medium, p38 MAPK competes with mAtg9 to interact with p38IP, and that inhibits the trafficking of mAtg9 and autophagy (Webber and Tooze, 2010). Therefore, Spt20 is able to regulate its effectors through physical interactions, which might be conserved between yeast and mammals.

Besides Spt20, transcription-independent functions have been reported for other SAGA subunits. For instance, ataxin-7 is a human homolog of yeast Sgf73, a subunit belonging to the histone deubiquitylation module of SAGA (Köhler et al., 2010). Ataxin-7 shuttles between the nucleus and cytoplasm during the cell cycle. Cytoplasmic ataxin-7 is associated with microtubules and enhances the stability of microtubule filaments (Nakamura et al., 2012). Tra1 is the largest component of the SAGA complex. Tra1 has been identified as a subunit of a novel complex called ASTRA (for ‘assembly of Tel, Rvb and Atm-like kinase’), suggesting that Tra1 has roles that are independent of SAGA (Shevchenko et al., 2008). In the future, it will be interesting to investigate whether other subunits of SAGA can play transcription-independent roles, especially in different cellular compartments outside the nucleus.

In summary, our work unveils transcriptional-dependent and -independent roles of Spt20 in septin ring assembly. The finding not only advances our understanding of the mechanism underlying the organization of high-order septin structures, but also highlights the multifaceted regulation of one process by a SAGA subunit.

MATERIALS AND METHODS

Yeast strains and media

S. pombe strains used in this study are listed in supplementary material Table S1 and were grown in yeast extract medium with supplements (YES) or Edinburgh minimal medium (EMM2) supplemented with appropriated amino acids as described previously (Forsburg and Rhind, 2006). The medium was supplemented with 15 μM thiamine as indicated, to repress expressions driven by *nmt1*$^+$, *nmt41*$^+$ or *nmt81*$^+$ promoters (Basi et al., 1993). Gene deletion and tagging were performed by homologous recombination using a plasmid-based method (Gregan et al., 2006). In brief, pCloneHyg1 was used to delete *spt20*$^+$, *gcn5*$^+$, *ubp8*$^+$, *spt8*$^+$, *spt7*$^+$ or *mid2*$^+$ by using a *hphMX4* or *kanMX4* deletion cassette. pCloneNat1 was used to delete *spn2*$^+$ by using a *natMX4* deletion cassette. *HphMX4* of pCloneHyg1 was replaced by *ura4*$^+$, and the derived plasmid (pCloneUra4) was used to delete *spn2*$^+$ or *mid2*$^+$ by *ura4*$^+$. $mCherry_3$ was inserted into pCloneUra4, and the derived plasmid was used to fuse $mCherry_3$ at the endogenous C-terminus of *spt20*$^+$. Similarly, single mCherry or GFP was fused at the endogenous C-terminus of *mid2*$^+$. Identities of strains, either constructed in this study or purchased from Bioneer and YGRC, were verified by PCR analysis.

Microscopy

Cells were grown in YES or EMM2 medium at 32℃ until the exponential stage and collected. To count the number of septa, cells were stained by 100 ng/ml Calcofluor White stain (18909, Sigma-Aldrich, St Louis, MO). To observe cells in Fig. 5, cells were fixed in cold 100% ethanol for 30 min before imaging. Images in Fig. 5A and Fig. 7B were taken at 23℃ through a Plan-Apochromat 63×/1.40 NA Oil DIC M27 objective using a Zesis LSM710 confocal microscope equipped with a 488-nm argon laser and AxioCam camera (Carl Zeiss AG, Oberkochen, Germany). Images in Fig. 5A were acquired by taking five images

Journal of Cell Science (2014) 127, 4024–4036 doi:10.1242/jcs.151910

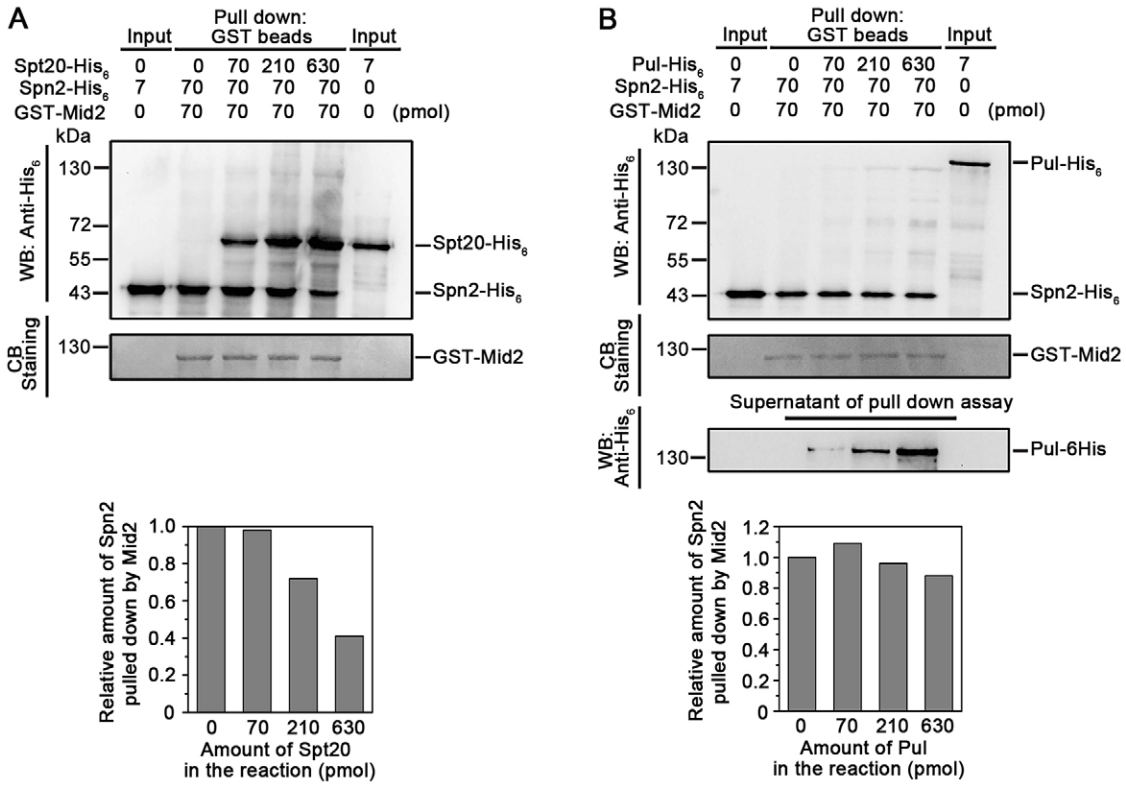

Fig. 8. Spt20 and Spn2 bind with Mid2 in a competitive manner. Result of a pulldown assay to examine the competitive binding of Spn2–His_6 and Spt20–His_6 to GST–Mid2. 70 pmol of GST–Mid2 was immobilized on GST beads, and was mixed with 70 pmol of Spn2–His_6 and increasing amounts of Spt20–His_6 (A) or Pul–His_6 (B). After the GST beads were thoroughly washed, proteins conjugated to the beads were detected by western blotting (WB) using anti-His_6 antibody. Coomassie Blue (CB) staining of GST–Mid2 is also shown. Pul–His_6 in the supernatant of pulldown assay was detected by western blotting using anti-His_6 antibody. The amount of Spn2 pulled down by Mid2 was quantified and shown in the bottom panel. The amount of Spn2 pulled down in the absence of Spt20 or Pul was designated as 1.

along the *z*-axis at 930-nm intervals. Images were analyzed by ZEN 2009 light edition software. FRET analysis in Fig. 5B was carried out with an IX71 TIRF microscope with an Apo N 60×/1.49 NA Oil objective (Olympus, Tokyo, Japan). GFP was excited with the 488-nm laser channels. Emission fluorescence intensity data was obtained at 500–540 nm (GFP) and 590–740 nm (mCherry). GFP and mCherry emission signals were captured by EMCCD (X-6035, Andor Technology, Belfast, Northern Ireland). FRET is indicated as the relative increase in mCherry emission following photobleaching of GFP (R_0 of the FRET pair is around 5 nm). The imaging system was controlled by the ANDOR SOLIS software. DIC, green and red fluorescence images of rest cells were captured by an UPlanFL N 100×/1.30 NA oil objective at room temperature using an IX51 inverted fluorescence microscope (Olympus). Images were analyzed by DP2-BSW software.

Flow cytometry

1×10^7–2×10^7 exponentially growing cells were harvested and fixed in 70% (v/v) cold ethanol for 1 h at 4℃. Then the cells were resuspended in 0.5 ml of 50 mM sodium citrate containing 0.1 mg/ml RNase A and were incubated at 37℃ for 2 h. Cells were briefly sonicated, and stained with 4 µg/ml Propidium Iodide at room temperature for 15 min. 10,000 cells were measured by a FACS Calibur flow cytometer (Becton Dickinson, Franklin Lakes, NJ, USA) and data were analyzed by Flowjo 2.0.

Real-time PCR

Total RNAs were prepared from exponentially growing cells by using RiboPure™-Yeast Kit (AM1926, Life Technologies, Carlsbad, CA, USA) and reverse transcribed to cDNAs by SYBR Premix Ex *Taq*II (RR820A, Takara, Dalian, China). Real-time PCR was performed by using a LightCycler 480 II Real-Time PCR System (Roche Applied Science, Penzberg, Upper Bavaria, Germany) with an initial step at 95℃ for 3 min followed by 40 cycles at 95℃ for 5 s, and 60℃ for 20 s. The threshold cycle (C_T) was determined automatically by the instrument and then normalized to the value for *act1*$^+$ by the following equation: $\Delta C_T = C_T$ (gene of interest) $- C_T$(*act1*$^+$). The relative level was calculated as $2^{-\Delta CT}$. The reactions for each sample were performed in triplicate. Primers are listed in supplementary material Table S2.

GST pulldown assay

GST and GST–Spt20 fusion proteins were separately expressed in bacteria and purified by a GST system (GE Healthcare, Piscataway, NJ, USA). N-terminal HA-tagged Spn1, Spn2, Spn4 or Mid2 was produced *in vitro* using the TNT T7 Quick coupled transcription/translation system (L1170, Promega, Madison, WI). C-terminal His_6-tagged Spt20 was expressed and purified using the pET system (Merck KGaA, Darmstadt, Germany). An equal amount of GST or GST–Spt20 was immobilized on the beads and incubated with HA-tagged proteins or Spt20–His_6 in NETN buffer (50 mM Tris-HCl pH 7.5, 200 mM NaCl, 2 mM EDTA and 0.1% NP-40) at 4℃ for 4 h. Bead-conjugated complexes were washed with Buffer H (20 mM Hepes pH 7.5, 50 mM KCl, 20% glycerol, 0.1% NP-40 and 0.007% β-mercaptoethanol) thoroughly, boiled in SDS-gel loading buffer and then subjected to western blotting analysis using anti-HA (M20013, Abmart, Shanghai, China) or anti-His_6 (M30111, Abmart) antibodies. Western blot data was imaged by the GeneGnome Bio Imaging System (Syngene, Cambridge, UK). For the competitive binding assay, GST–Mid2 was expressed and purified by using the GST system, and Spt20–His_6, Spn2–His_6 and Pul–His_6 by using the pET system. Amounts of proteins were quantified by SDS-PAGE using BSA as a control. Immobilized GST–Mid2 was incubated with Spn2–His_6 and increasing amounts of Spt20–His_6 or Pul–His_6 at 4℃ for

4 h. Bead-conjugated proteins were washed, boiled and subjected to western blotting using anti-His_6 antibody. Intensities of the bands were quantified with ImageJ.

Whole-cell extract and co-immunoprecipitation assay

Three tandem FLAG tags were fused at N-terminus of *spn1*$^+$, *spn2*$^+$, *spn3*$^+$, *spn4*$^+$ or *mid2*$^+$ open reading frames (ORFs) and cloned into the pREP1 vector (Maundrell, 1993). Five tandem HA tags were fused at C-terminus of *spt20*$^+$ ORF and cloned into the pJR2-41U vector (Moreno et al., 2000). Cells were co-transformed with pJR2-41U-Spt20-HA and pREP1 plasmid expressing one of the FLAG-tagged septins or Mid2. As a negative control, cells were co-transformed with pJR2-41U-Spt20-HA and pREP1-FLAG. Transformants were grown to the exponential phase in EMM2 medium without leucine and uracil and harvested. Cells were broken by glass beads in lysis buffer (50 mM Tris-HCl pH 7.5, 150 mM NaCl, 5 mM EDTA, 10% glycerol and 1 mM PMSF) and supernatant were collected as whole-cell extract after centrifugation. Extracts were pre-cleared with protein A/G plus agarose beads (sc-2003, Santa Cruz Biotechnology, Dallas, Texas, USA) at 4℃ for 45 min and were immunoprecipitated with anti-FLAG M2 affinity beads (A2220, Sigma-Aldrich). The bead-conjugated complexes were washed with lysis buffer, boiled in SDS-gel loading buffer and subjected to western blotting with anti-HA antibody. To assess the amounts of GFP-tagged proteins, the indicated strains were grown in YES medium until the exponential stage and were harvested for the whole-cell extract as described above. Extracts were subject to western blotting analysis by using anti-GFP antibody (M20004, Abmart). Histone H3 (07-690, Millipore, Billerica, MA, USA) in the extracts was blotted as a loading control.

Acknowledgements

We thank Quanwen Jin (School of Life Science, Xiamen University, China) for providing valuable strains, and Rolf Sternglanz (Department of Biochemistry and Cell Biology, Stony Brook University, USA) for his valuable comments on the manuscript.

Competing interests

The authors declare no competing interests.

Author contributions

B.L. designed and performed biochemical experiments; N.Z. designed and performed microscopy experiments; Y.G. assisted in experiments; W.Z. and Y.T. performed the FRET experiments; Y.Y. and H.L. designed and supervised the project; B.L. and Y.Y. wrote the manuscript. All authors reviewed and approved the manuscript.

Funding

This work was supported by National Program on the Key Basic Research Project (973 Program) [grant number 2009CB825601 to H.L.]; the National Natural Science Foundation of China [grant numbers 91129730 and 21132004 to H.L., 31200961 to Y.Y., 11274076 to Y.T.], the program 863 [grant numbers 2014AA021301 and 2013AA102803B to H.L.]; and the Specialized Research Fund for the Doctoral Program of Higher Education [grant numbers 20110071130007 to H.L., 20120071120010 to Y.Y.].

Supplementary material

Supplementary material available online at
http://jcs.biologists.org/lookup/suppl/doi:10.1242/jcs.151910/-/DC1

References

Alonso-Nuñez, M. L., An, H., Martín-Cuadrado, A. B., Mehta, S., Petit, C., Sipiczki, M., del Rey, F., Gould, K. L. and de Aldana, C. R. (2005). Ace2p controls the expression of genes required for cell separation in Schizosaccharomyces pombe. *Mol. Biol. Cell* **16**, 2003-2017.

An, H., Morrell, J. L., Jennings, J. L., Link, A. J. and Gould, K. L. (2004). Requirements of fission yeast septins for complex formation, localization, and function. *Mol. Biol. Cell* **15**, 5551-5564.

Basi, G., Schmid, E. and Maundrell, K. (1993). TATA box mutations in the Schizosaccharomyces pombe nmt1 promoter affect transcription efficiency but not the transcription start point or thiamine repressibility. *Gene* **123**, 131-136.

Batta, G., Szilagyi, Z., Laczik, M. and Sipiczki, M. (2009). The involvement of the Schizosaccharomyces pombe sep9/spt8 gene in the regulation of septum cleavage. *FEMS Yeast Res.* **9**, 757-767.

Berlin, A., Paoletti, A. and Chang, F. (2003). Mid2p stabilizes septin rings during cytokinesis in fission yeast. *J. Cell Biol.* **160**, 1083-1092.

Espinosa, M. C., Rehman, M. A., Chisamore-Robert, P., Jeffery, D. and Yankulov, K. (2010). GCN5 is a positive regulator of origins of DNA replication in Saccharomyces cerevisiae. *PLoS ONE* **5**, e8964.

Forsburg, S. L. and Rhind, N. (2006). Basic methods for fission yeast. *Yeast* **23**, 173-183.

García-Oliver, E., García-Molinero, V. and Rodríguez-Navarro, S. (2012). mRNA export and gene expression: the SAGA-TREX-2 connection. *Biochim. Biophys. Acta* **1819**, 555-565.

Grant, P. A., Duggan, L., Côté, J., Roberts, S. M., Brownell, J. E., Candau, R., Ohba, R., Owen-Hughes, T., Allis, C. D., Winston, F. et al. (1997). Yeast Gcn5 functions in two multisubunit complexes to acetylate nucleosomal histones: characterization of an Ada complex and the SAGA (Spt/Ada) complex. *Genes Dev.* **11**, 1640-1650.

Gregan, J., Rabitsch, P. K., Rumpf, C., Novatchkova, M., Schleiffer, A. and Nasmyth, K. (2006). High-throughput knockout screen in fission yeast. *Nat. Protoc.* **1**, 2457-2464.

Gulli, M. P., Faubladier, M., Sicard, H. and Caizergues-Ferrer, M. (1997). Mitosis-specific phosphorylation of gar2, a fission yeast nucleolar protein structurally related to nucleolin. *Chromosoma* **105**, 532-541.

Helmlinger, D. (2012). New insights into the SAGA complex from studies of the Tra1 subunit in budding and fission yeast. *Transcription* **3**, 13-18.

Helmlinger, D., Marguerat, S., Villén, J., Swaney, D. L., Gygi, S. P., Bähler, J. and Winston, F. (2011). Tra1 has specific regulatory roles, rather than global functions, within the SAGA co-activator complex. *EMBO J.* **30**, 2843-2852.

Hickman, M. J., Spatt, D. and Winston, F. (2011). The Hog1 mitogen-activated protein kinase mediates a hypoxic response in Saccharomyces cerevisiae. *Genetics* **188**, 325-338.

Joberty, G., Perlungher, R. R., Sheffield, P. J., Kinoshita, M., Noda, M., Haystead, T. and Macara, I. G. (2001). Borg proteins control septin organization and are negatively regulated by Cdc42. *Nat. Cell Biol.* **3**, 861-866.

Kang, P. J., Hood-DeGrenier, J. K. and Park, H. O. (2013). Coupling of septins to the axial landmark by Bud4 in budding yeast. *J. Cell Sci.* **126**, 1218-1226.

Köhler, A., Zimmerman, E., Schneider, M., Hurt, E. and Zheng, N. (2010). Structural basis for assembly and activation of the heterotetrameric SAGA histone H2B deubiquitinase module. *Cell* **141**, 606-617.

Lee, P. R., Song, S., Ro, H. S., Park, C. J., Lippincott, J., Li, R., Pringle, J. R., De Virgilio, C., Longtine, M. S. and Lee, K. S. (2002). Bni5p, a septin-interacting protein, is required for normal septin function and cytokinesis in Saccharomyces cerevisiae. *Mol. Cell. Biol.* **22**, 6906-6920.

Lenstra, T. L., Benschop, J. J., Kim, T., Schulze, J. M., Brabers, N. A., Margaritis, T., van de Pasch, L. A., van Heesch, S. A., Brok, M. O., Groot Koerkamp, M. J. et al. (2011). The specificity and topology of chromatin interaction pathways in yeast. *Mol. Cell* **42**, 536-549.

Martín-Cuadrado, A. B., Morrell, J. L., Konomi, M., An, H., Petit, C., Osumi, M., Balasubramanian, M., Gould, K. L., Del Rey, F. and de Aldana, C. R. (2005). Role of septins and the exocyst complex in the function of hydrolytic enzymes responsible for fission yeast cell separation. *Mol. Biol. Cell* **16**, 4867-4881.

Matsuyama, A., Arai, R., Yashiroda, Y., Shirai, A., Kamata, A., Sekido, S., Kobayashi, Y., Hashimoto, A., Hamamoto, M., Hiraoka, Y. et al. (2006). ORFeome cloning and global analysis of protein localization in the fission yeast Schizosaccharomyces pombe. *Nat. Biotechnol.* **24**, 841-847.

Maundrell, K. (1993). Thiamine-repressible expression vectors pREP and pRIP for fission yeast. *Gene* **123**, 127-130.

Milgrom, E., West, R. W., Jr, Gao, C. and Shen, W. C. (2005). TFIID and Spt-Ada-Gcn5-acetyltransferase functions probed by genome-wide synthetic genetic array analysis using a Saccharomyces cerevisiae taf9-ts allele. *Genetics* **171**, 959-973.

Moreno, M. B., Durán, A. and Ribas, J. C. (2000). A family of multifunctional thiamine-repressible expression vectors for fission yeast. *Yeast* **16**, 861-872.

Mostowy, S. and Cossart, P. (2012). Septins: the fourth component of the cytoskeleton. *Nat. Rev. Mol. Cell Biol.* **13**, 183-194.

Nagy, Z., Riss, A., Romier, C., le Guezennec, X., Dongre, A. R., Orpinell, M., Han, J., Stunnenberg, H. and Tora, L. (2009). The human SPT20-containing SAGA complex plays a direct role in the regulation of endoplasmic reticulum stress-induced genes. *Mol. Cell. Biol.* **29**, 1649-1660.

Nakamura, Y., Tagawa, K., Oka, T., Sasabe, T., Ito, H., Shiwaku, H., La Spada, A. R. and Okazawa, H. (2012). Ataxin-7 associates with microtubules and stabilizes the cytoskeletal network. *Hum. Mol. Genet.* **21**, 1099-1110.

Oegema, K., Savoian, M. S., Mitchison, T. J. and Field, C. M. (2000). Functional analysis of a human homologue of the Drosophila actin binding protein anillin suggests a role in cytokinesis. *J. Cell Biol.* **150**, 539-552.

Onishi, M., Koga, T., Hirata, A., Nakamura, T., Asakawa, H., Shimoda, C., Bähler, J., Wu, J. Q., Takegawa, K., Tachikawa, H. et al. (2010). Role of septins in the orientation of forespore membrane extension during sporulation in fission yeast. *Mol. Cell. Biol.* **30**, 2057-2074.

Pan, F., Malmberg, R. L. and Momany, M. (2007). Analysis of septins across kingdoms reveals orthology and new motifs. *BMC Evol. Biol.* **7**, 103.

Pan, X., Lei, B., Zhou, N., Feng, B., Yao, W., Zhao, X., Yu, Y. and Lu, H. (2012). Identification of novel genes involved in DNA damage response by screening a genome-wide Schizosaccharomyces pombe deletion library. *BMC Genomics* **13**, 662.

Petit, C. S., Mehta, S., Roberts, R. H. and Gould, K. L. (2005). Ace2p contributes to fission yeast septin ring assembly by regulating mid2+ expression. *J. Cell Sci.* **118**, 5731-5742.
Qiu, W., Neo, S. P., Yu, X. and Cai, M. (2008). A novel septin-associated protein, Syp1p, is required for normal cell cycle-dependent septin cytoskeleton dynamics in yeast. *Genetics* **180**, 1445-1457.
Shevchenko, A., Roguev, A., Schaft, D., Buchanan, L., Habermann, B., Sakalar, C., Thomas, H., Krogan, N. J., Shevchenko, A. and Stewart, A. F. (2008). Chromatin Central: towards the comparative proteome by accurate mapping of the yeast proteomic environment. *Genome Biol.* **9**, R167.
Sipiczki, M. (2007). Splitting of the fission yeast septum. *FEMS Yeast Res.* **7**, 761-770.
Sterner, D. E., Grant, P. A., Roberts, S. M., Duggan, L. J., Belotserkovskaya, R., Pacella, L. A., Winston, F., Workman, J. L. and Berger, S. L. (1999). Functional organization of the yeast SAGA complex: distinct components involved in structural integrity, nucleosome acetylation, and TATA-binding protein interaction. *Mol. Cell. Biol.* **19**, 86-98.
Tasto, J. J., Morrell, J. L. and Gould, K. L. (2003). An anillin homologue, Mid2p, acts during fission yeast cytokinesis to organize the septin ring and promote cell separation. *J. Cell Biol.* **160**, 1093-1103.
Webber, J. L. and Tooze, S. A. (2010). Coordinated regulation of autophagy by p38alpha MAPK through mAtg9 and p38IP. *EMBO J.* **29**, 27-40.
Wu, P. Y. and Winston, F. (2002). Analysis of Spt7 function in the Saccharomyces cerevisiae SAGA coactivator complex. *Mol. Cell. Biol.* **22**, 5367-5379.
Yu, Y., Eriksson, P., Bhoite, L. T. and Stillman, D. J. (2003). Regulation of TATA-binding protein binding by the SAGA complex and the Nhp6 high-mobility group protein. *Mol. Cell. Biol.* **23**, 1910-1921.
Zohn, I. E., Li, Y., Skolnik, E. Y., Anderson, K. V., Han, J. and Niswander, L. (2006). p38 and a p38-interacting protein are critical for downregulation of E-cadherin during mouse gastrulation. *Cell* **125**, 957-969.